Geomechanics and Engineering, *Vol. 41, No. 2 (2025) 255-264*
https://doi.org/10.12989/gae.2025.41.2.255

Research and application of a mechanical method combined with chemical grouting for correcting settlement and deviation in double block ballastless track structure

Zhipeng Su*[1], Junhua Xiao[1a], Xi Yang[2b] and Lingzi Zhao[2c]

[1]*Shanghai Key Laboratory of Rail Infrastructure Durability and System Safety, Tongji University, No.1239, Siping Road, Yangpu District, Shanghai, China*
[2]*Shanghai Shen Yuan Geotechnical Engineering Co., Ltd, No.1368, South Xizang Road, Huangpu District, Shanghai, China*

(*Received November 28, 2024, Revised March 12, 2025, Accepted April 9, 2025*)

Abstract. This paper presents a new method to address subgrade settlement and alignment deviations in double-block ballastless tracks for high-speed railways. The method focuses on minimizing damage to the track structure during the lifting and rectification of the double-block ballastless track in short-length subgrade sections. A finite element model (FEM) was developed to analyze key construction parameters, including jack spacing and dissociation length. Numerical simulations determined that a 3 m jack spacing is optimal, as increasing it to 5 m results in a 20%–32% increase in jacking force. Additionally, a 31 m dissociation length effectively reduces stress on the track structure while maintaining construction efficiency. The multi-point horizontal thrust correction method was validated, achieving a maximum lift of 39.5 mm and a maximum deviation correction of 4 mm, without inducing structural cracking. Post-construction evaluations confirmed significant enhancements in track smoothness and alignment. Dynamic inspection data indicated a >60% reduction in peak-to-valley values, horizontal displacement, and vertical acceleration. Furthermore, real-time displacement monitoring verified that lateral and vertical movements remained below 0.2 mm and 0.3 mm, respectively, ensuring compliance with high-speed railway safety standards. These findings demonstrate that the proposed mechanical lifting and chemical grouting technique effectively mitigates subgrade settlement and track misalignment. The proposed method has been successfully applied to the Beijing-Guangzhou railway, demonstrating effective solutions for subgrade settlement and alignment deviations in the maintenance phase. As a result, the track smoothness was successfully restored, meeting the operational requirements for increased train speed.

Keywords: ballastless track; correction; high-speed railway; lifting

1. Introduction

Foundation deformation can lead to a variety of engineering issues and significantly impact on structural safety. As a result, geotechnical experts have undertaken extensive theoretical and practical research in this area, addressing the issue through geosynthetics (Zamani *et al*. 2023) and grouting (Bian *et al*. 2021). Research on foundation diseases has yielded significant results in civil engineering, particularly in the context of stress caused by such issues (Amornfa *et al*. 2023). As road and rail transportation systems continue to evolve, methods for detecting and analyzing slope stability are constantly advancing. These advancements include the use of numerical simulations to evaluate slope stability, the analysis of soil structure parameters through microscopic testing, the application of dynamic testing to monitor and predict changes in roadbed stability, and the integration of big data models to enhance the safety and efficiency of railway operations and maintenance. (Hu *et al*. 2023, Chen *et al*. 2024, Zuo *et al*. 2022, Ghofrani *et al*. 2018). Simultaneously, the deformation and settlement of high-speed railway tracks have garnered increasing attention (Hadi *et al*. 2023, Charoenwong *et al*. 2022, Paixão *et al*. 2015).

Ballastless track is characterized by high smoothness, integrity, stability, and reduced maintenance requirements. Giunta and Praticò (2017) conducted a cost analysis comparing different track solutions. Ballastless track offers advantages such as an extended service life, low maintenance costs, and high lateral stability. However, it may lead to uneconomical maintenance and renewal costs over extended life span. Ballastless track is the primary track structure used in China's high-speed railway system. High-speed rail (HSR) ballastless track defects are influenced by various factors, including the track structure, temperature fluctuations, water ingress, train loads, deformation of the underlying foundation, and construction quality (Dong *et al*. 2022). Settlement amplitude and settlement wavelength of the subgrade have significant effects on track deformation (Cui *et al*. 2017). The ballastless track structure of individual road base sections

*Corresponding author, Ph.D. Student
E-mail: Zhipeng_Su@foxmail.com
[a] Professor
[b]Engineer
[c]Engineer

ISSN: 2005-307X (Print), 2092-6219 (Online)

Table 1 Calculation model material parameter table

Name	Poisson ratio	Density (kg/m^3)	Constitutive model	Elastic modulus (GPa)	Cohesion (kPa)	Friction angle (°)
rail	0.3	7850	Elastic	210.0	-	-
track slab	0.2	2500	Elastic	32.5	-	-
supporting layer	0.2	2500	Elastic	30.0	-	-
subgrade	0.3	1950	MC	0.19	5	40

may experience horizontal displacement, which can lead to significant lateral irregularities in the track. This phenomenon negatively impacts normal operation and accelerates the deformation and failure of various track components (Liu *et al*. 2021). Subgrade settlement and track deviation have become prevalent defects, impacting track smoothness, driving safety, and riding comfort. When settlement and horizontal deviation surpass the adjustment limit of fasteners, it becomes necessary to employ track structure lifting and correction technology to rectify these issues. This technology primarily utilizes mechanical or grouting lifting methods to raise the detached upper track structure to the target elevation. Horizontal thrust is then applied to correct track deviation, followed by grouting to fill the gaps created during the lifting process. Currently, this technology has been successfully applied to CRTSI, CRTSII, and CRTSIII slab ballastless tracks, as well as turnout of ballastless tracks for skylight operations (Zeng *et al*. 2022, Ren *et al*. 2021).

A high-speed railway implemented a double-block ballastless track structure. Subsidence and deviation were observed in the roadbed section, with a maximum settlement of 48 mm and a maximum deviation of 8 mm. Given that the affected section is only 21 m long, the stress on the track structure and the construction safety risks are significant when lifting and correcting the deviation. In-depth research into existing technical solutions, tailored to the specific characteristics of the project, is essential.

The double-block ballastless track poses significant challenges in regulating subgrade settlement and correcting track deviation, primarily due to its structural integrity and the millimeter-level precision required for maintenance. Key concerns include high safety risks, stringent quality control, and complex construction logistics. The short deviation correction section (21 m) requires substantial horizontal thrust, increasing the likelihood of structural cracks and stress concentration. Furthermore, the limited skylight operation time necessitates rapid yet precise execution, placing high demands on both technical expertise and construction management. To ensure successful implementation, three critical construction parameters must be determined: the maximum horizontal deviation correction thrust, the optimal spacing for horizontal jack placement, and the dissociation length of the high-closed layer. These parameters were optimized through simulation tests, enhancing construction efficiency while minimizing structural impact and safety risks.

This study aims to develop and validate an innovative lifting and rectification method to mitigate subgrade settlement and track deviation in double-block ballastless tracks used in high-speed railways. By integrating finite element modeling, mechanical lifting, horizontal correction, and chemical grouting, the research optimizes key construction parameters to enhance correction efficiency while minimizing structural impact. The findings provide a valuable reference for similar double-block ballastless track structure lifting and correction projects in roadbed sections.

2. Overall construction solution

Given the key challenges of the project and the need to minimize damage to the track structure, an integrated technical solution combining mechanical lifting and chemical grouting for double-block ballastless track was proposed and implemented in three stages:

The first stage primarily involves re-surveying the alignment and padding of the operation area, reinforcing the track slab in the correction zone with rebar, removing the sealing layer between the lines and shoulder side, excavating the lifting groove, and pouring horizontal reaction and limit piers.

The second stage primarily includes mechanical lifting of the track structure, horizontal correction, limit locking, and grouting to fill gaps. The correction and dissociation interface lies between the supporting layer and the graded crushed stone of the subgrade.

The third stage primarily involves chemical grouting and lifting of the settlement area, backfilling with graded crushed stone, re-casting the sealing layer, restoring caulking, and fine-tuning the track.

3. Numerical analysis of track deviation correction

The deviation correction length for this project is 21 m, with a maximum deviation of 8 mm, making it suitable for multi-point horizontal thrust correction.

According to the construction plan in Section 2, the horizontal deviation correction of the track structure in this project is performed using mechanical jacking. It is essential to calculate and estimate the required jacking force and the horizontal spacing of the jacks prior to construction. Based on practical experience, completing horizontal jacking without dissociation of the high closed layer between lines is challenging, and the dissociation length directly affects the construction time. Consequently, these parameters must be estimated in advance to ensure efficient project execution.

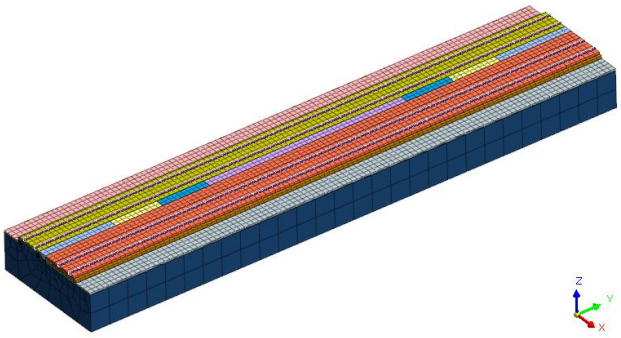

Fig. 1 Deviation correction calculation model diagram

Therefore a finite element refined static analysis numerical model is employed to conduct a regularity study, primarily aimed at determining the aboved three key construction parameters:

1) Maximum horizontal deviation correction thrust;
2) Horizontal jack arrangement spacing;
3) Dissociation length of the high closed layer between lines.

Using the numerical model, the influence of various construction parameters on the correction results was analyzed, and the optimal parameters were identified.

3.1 Computational model and material parameters

Finite element software was employed for numerical analysis. The rails, track plates, and support layers were simulated using elastic materials, while the subgrade was modeled using Mohr-Coulomb material. The selection of parameters for this material has been verified by scholars and accurately reflects the stress and deformation characteristics (Scheweiger *et al.* 2004, Nguyen *et al.* 2023, Song *et al.* 2024). The calculation parameters for the model presented in this paper are provided in Table 1.

The friction coefficient between the supporting layer and the roadbed significantly impacts the magnitude of the jacking force applied for correction (Ngamkhanong *et al.* 2021, Nobakht *et al.* 2022). Based on previous studies, this research assumed a friction coefficient of 0.5, which is consistent with engineering scenarios where the coefficient decreases due to jacking.

Based on the correction length of 21 m and the track size, a calculation model was established with dimensions of 56 m ×12.4 m ×5 m (length×width×height), shown in Fig. 1.

The center spacing between the upper and lower tracks is approximately 5 m. The track slab is 2.8 m wide and 0.24 m thick, the supporting layer is 3.4 m wide and 0.3 m thick, with a gravel subgrade at the base. Both the structure and subgrade are represented as solid hexahedral 3D units, comprising a total of 22,600 model units. Model boundary conditions are as follows: the bottom limits displacement in the X, Y, and Z directions; the ends limit normal displacement perpendicular to the free surface; and the upper part is modeled as a free surface.

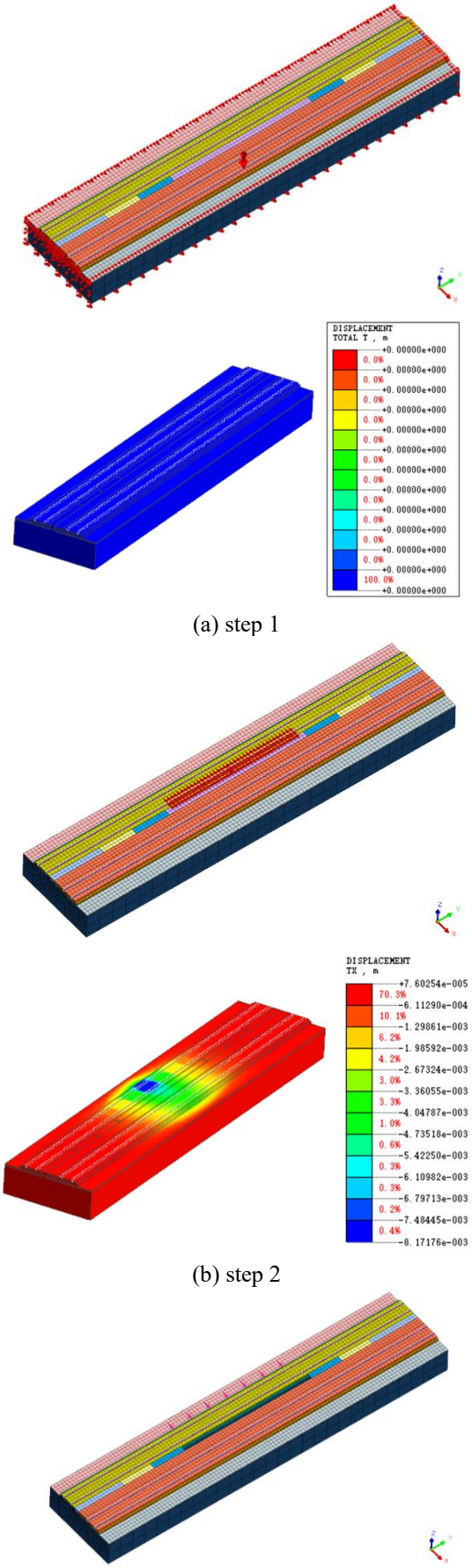

(a) step 1

(b) step 2

Fig. 2 Model status and horizontal displacement cloud diagram at each calculation step

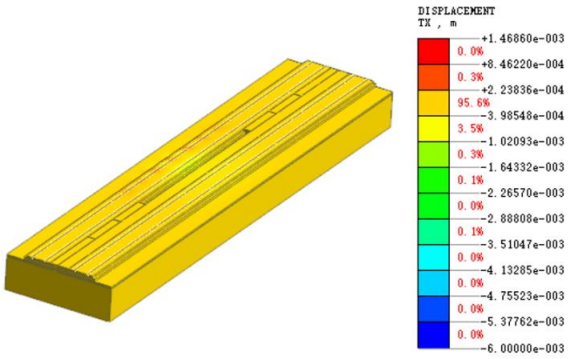

(c) step 3

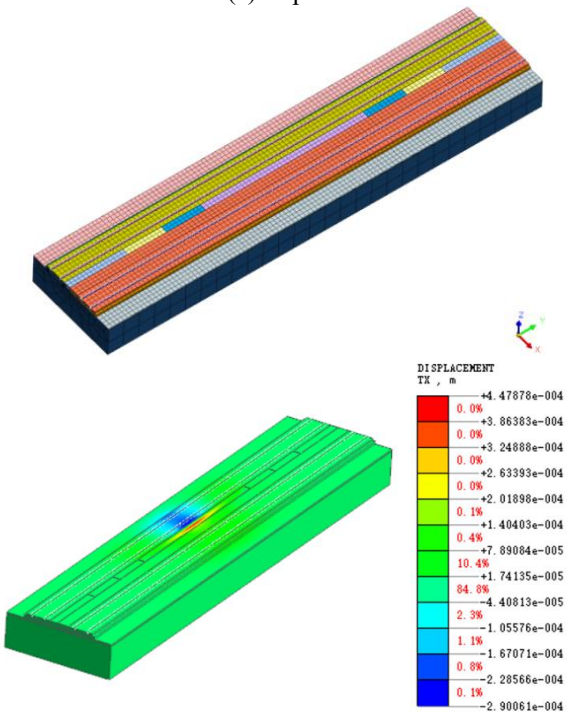

(d) step 4

Fig. 2 Continued-

3.2 Computational model Correction calculation steps

The correction length of the upward line is 21 m, and horizontal jacks with a spacing of 3 m are used to configure the supporting layer for correction. The sealing layer within the 21 m correction range, located between the upward and downward lines, is separated to facilitate gradual horizontal correction. The simulation steps for the calculation model are as follows,shown in Fig. 2:

1) Establish the overall self-stress balance of the model;

2) Apply forced displacement to simulate the existing offset;

3) Deactivate the inter-line supporting layer grid to simulate separation and apply concentrated force to model thrust correction;

4) Terminate the jacking process, allowing the structure to return to normal functionality.

The calculated deformation of the upward line indicates that track correction can be effectively achieved using the multi-point horizontal thrust method shown in Fig. 3. This

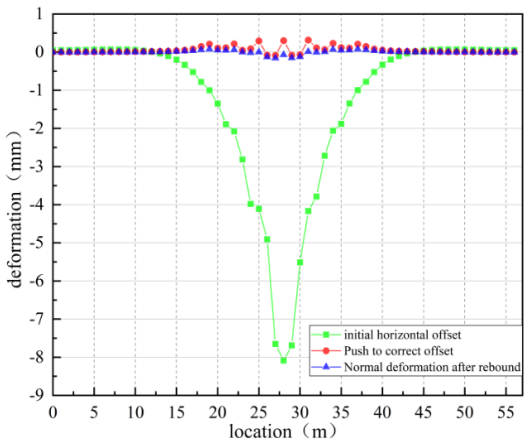

Fig. 3 Deformation diagram for each calculation step

Table 2 Calculation analysis table

Case No.	Jack spacing (m)	dissociation length (m)
A	3	21
B	3	31
C	3	41
D	5	21
E	5	31
F	5	41

approach demonstrates a strong correction effect, with minimal recovery rebound after correction, ensuring no significant impact on the overall correction results.

3.3 Analysis of construction parameter selection

To ensure effective construction, it is essential to determine the appropriate horizontal thrust arrangement spacing, jack spacing, and dissociation length of the high-sealing layer between the lines, as well as to identify the maximum horizontal thrust. The correction results are comprehensively evaluated by calculating jack spacings of 3 m and 5 m and total dissociation lengths of L= 21 m, L+2 ×5 m=31 m, and L+2×10 m=41 m. Differences in the jacking force and structural stress required to achieve the same correction effect under various construction parameters are compared and analyzed. The parameter combinations required for this study are calculated according to the A-F numbers, and the combinations are shown in Table 2.

The calculation and analysis table is as follows:

When the jack spacing is 3 m, seven jacks are arranged within the 21 m correction range. When the jack spacing is 5 m, five jacks are arranged within the same correction range. The arrangement of the jacks is illustrated in Fig. 4.

The statistical results, as shown in the following Table 3 and Fig. 5, indicate that when the jack spacing increases from 3 m to 5 meters, the jacking force at each point increases by 20% to 32% on average to achieve the same correction effect. When the jack spacing remains constant, increasing the dissociation length from 21 m to 31 m

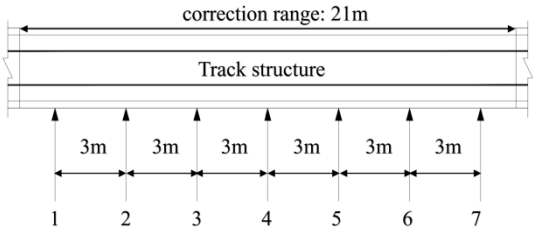

(a) 3 m spacing jack layout

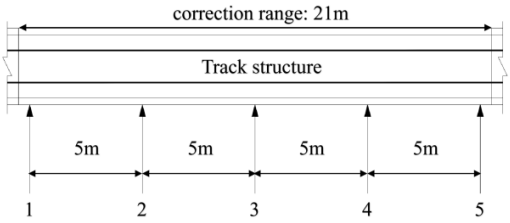

(b) 5 m spacing jack layout

Fig. 4 Layout diagram of jacks

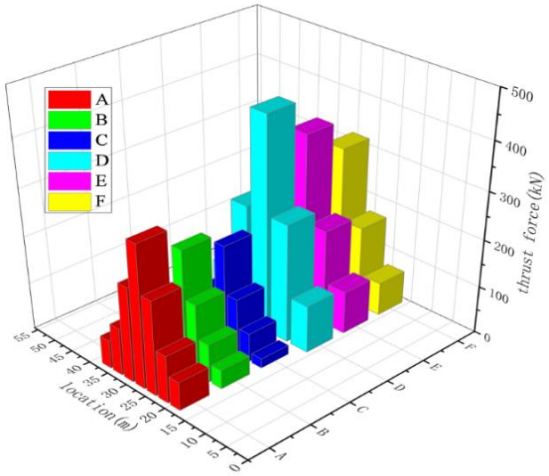

Fig. 5 Jacking force distribution of different construction parameters

Table 3 Jacking force distribution table unit(kN)

The jack serial number	A	B	C	D	E	F
1	60	40	20	100	90	70
2	100	80	60	250	200	170
3	200	150	120	450	380	320
4	300	250	220	250	200	170
5	200	150	120	100	90	70
6	100	80	60			
7	60	40	20			

reduces the jacking force per point by approximately 20% on average. Further increasing the dissociation length from 31 m to 41 m results in an average jacking force reduction of approximately 21% per point.

When the dissociation length is 21 m, the maximum effective stress in the X-axis direction of the supporting layer reaches 1.32 MPa. For a dissociation length of 31 m,

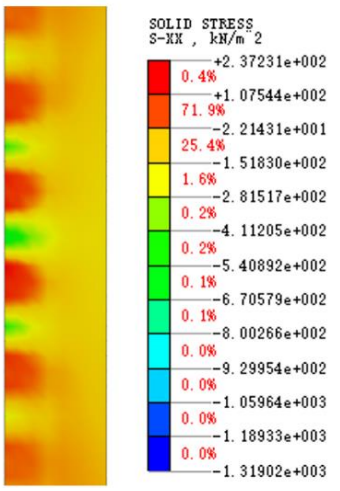

(a) 21 m dissociation length

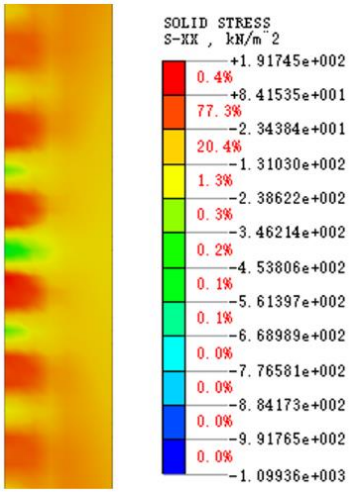

(b) 31 m dissociation length

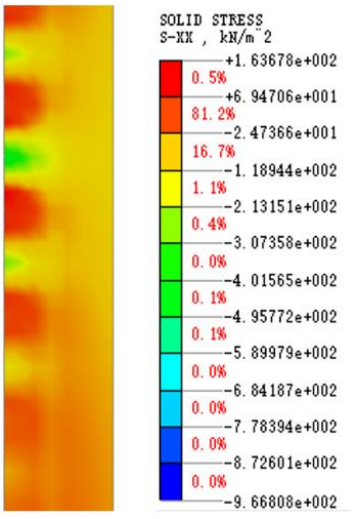

(c) 41 m dissociation length

Fig. 6 Effective stress cloud diagram in the X-axis direction at different dissociation length

this value decreases to 1.10 MPa, and for 41 m, it further decreases to 0.97 MPa shown in Fig. 6. These results indicate that a longer dissociation length is more beneficial for protecting the track structure during deviation

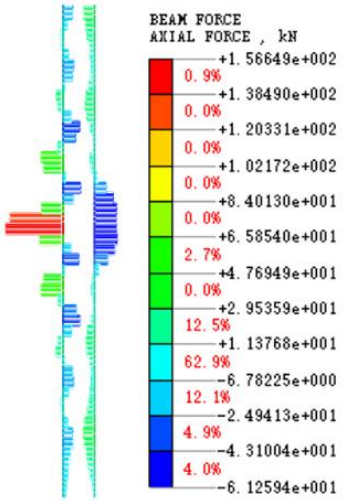

(a) 3 m jack spacing

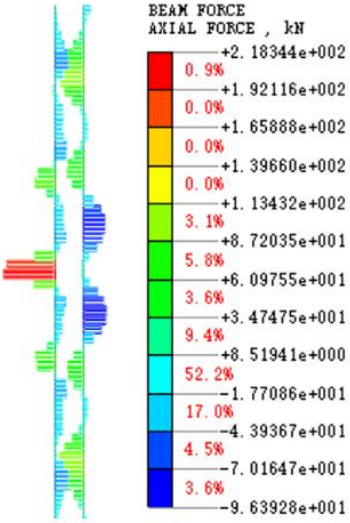

(b) 5 m jack spacing

Fig. 7 Track stress cloud diagram in X-axis direction with different jack spacing

correction. However, separation construction during the limited skylight period requires significant manpower and time, reducing overall efficiency. Therefore, a dissociation length of 31 m is selected as the optimal configuration.

When the dissociation length is 31 m, the maximum force on the track in the X-axis direction is 156.6 kN for a jack spacing of 3 m and 218.3 kN for a jack spacing of 5 m shown in Fig. 7. This demonstrates that a jack spacing of 3 m not only reduces the jacking force and minimizes disturbance to the supporting layer but also decreases uneven force on the track. Therefore, a jack spacing of 3 m is the most suitable configuration.

In summary, with a maximum correction amount of 8 mm and a correction length of 21 m, increasing the jack spacing from 3 m to 5 m results in a 20% to 32% average increase in the jacking force required at each point to achieve the same correction effect. For every 5 m increase in the separation length on both sides of the correction range, the jacking force at each point decreases by approximately 20% on average. Considering structural

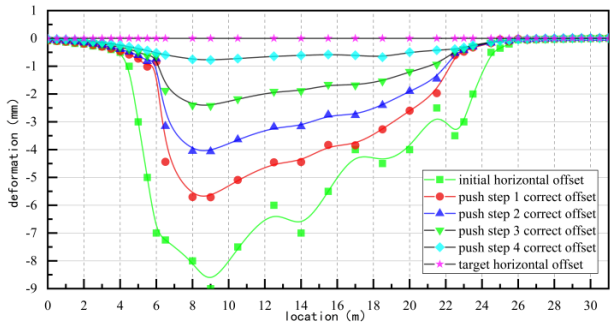

Fig. 8 Step-by-step correction process linear horizontal curve

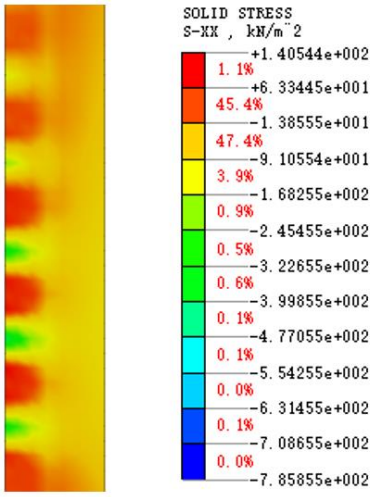

Fig. 9 Effective stress cloud diagram in the X-axis direction of the supporting layer during correction

stress and construction efficiency, the construction parameters are defined as follows:

1) A correction amount of ⩽8 mm corresponds to a thrust of ⩽300 kN, which is manageable by conventional jack equipment;

2) The optimal spacing for horizontal correction jacks is 3 m;

3) The ideal separation length on both sides of the correction range is 5 m.

3.4 Simulated construction effect

A finite element model reflecting the actual horizontal deviation of the project was developed. Seven jacks were arranged on the correction side, with a jack spacing of 3 m. A separation length of 5 m was added to each side, in addition to the correction length, resulting in a total separation length of 31 m.

As shown in Fig. 8 below, the correction was performed in four steps according to the actual working conditions, with the correction amount not exceeding 3 mm at each step. The target line shape was gradually restored.

The jacks were arranged as depicted in Fig. 4(a) above. The thrusts applied by jacks No.1 through No.7 were 250 kN, 300 kN, 250 kN, 150 kN, 100 kN, 50 kN, and 0 kN, respectively. During the correction, the maximum effective

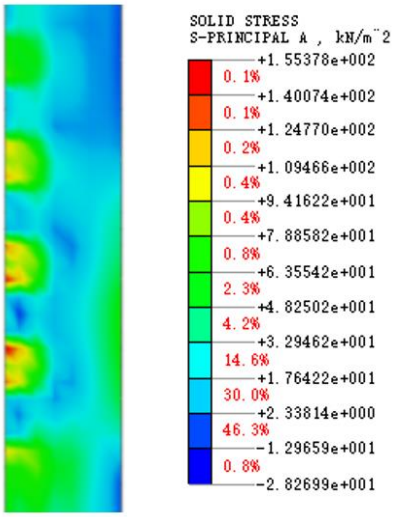

Fig. 10 Maximum tensile stress cloud diagram of the supporting layer during correction

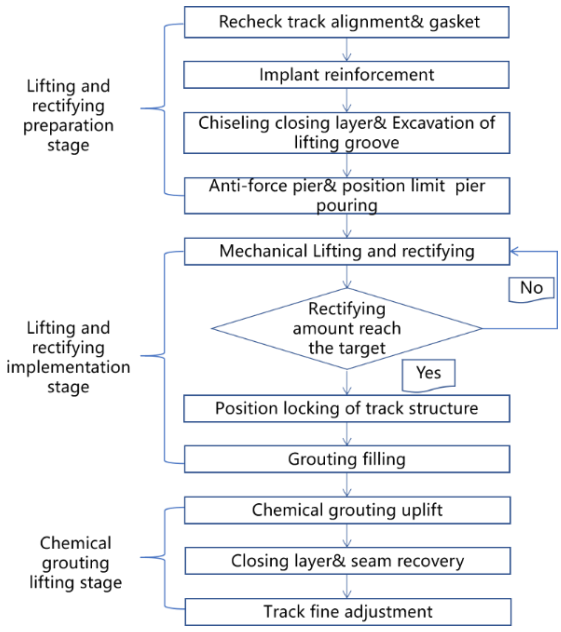

Fig. 11 Lifting and rectifying construction process of ballastless track structure

stress in the X-axis direction of the supporting layer was 0.78 MPa, while the maximum tensile stress was 0.16 MPa, both of which met the structural bearing requirements, as shown in Figs. 9 and 10. The correction process will not cause cracking or crushing of the ballastless track concrete.

4. Construction technology

4.1 Construction process

Based on the three key construction parameters derived from the simulation calculations in Chapter 3, construction tests were carried out. The optimized construction process and key procedures are illustrated in Fig. 11.

4.2 Construction quality control of key process

4.2.1 Implant reinforcement

The interface of rectification and dissociation lies between the supporting layer and the gravel subgrade. Steel bars are embedded to connect the track slab and supporting layer, ensuring the displacement synchronization of the track structure during the lifting and rectification process. After drilling, the hole should be thoroughly cleaned and dried, and then injected with reinforcement adhesive, starting from the bottom of the hole up to 2/5 of its depth. During reinforcement installation, the bars should be rotated slowly.

4.2.2 Chiseling sealing layer& Excavation of lifting groove

Based on the simulation results in Chapter 3, the sealing layer to be chiseled extends 5 m from both ends of the rectification area, with a total length of 31 m. In the rectification area, lifting grooves are positioned at 3 m intervals along the supporting layer on both sides of the track. Six lifting grooves are placed in the rectification area, with a total of 12 grooves prepared for mechanical lifting. The lifting groove depth is 40 cm below the supporting layer. In the longitudinal direction, the groove measures 80 cm in length and 140 cm in width. Upon completion of the lifting groove excavation, the bottom is leveled and hardened with concrete to prepare for jack placement.

4.2.3 Anti-force pier& position limit pier pouring

Based on the simulation results in Chapter 3 and construction tests, the spacing of the anti-force pier and position limit pier is 3 m along the track. The section dimensions of the anti-force pier are 1.2 m by 1.2 m, with a pier height of 0.4 m. The position limit pier is a structural element that does not provide corrective reaction force, with section dimensions of 0.8 m by 0.6 m and a pier height of 0.4 m.

4.2.4 Mechanical Lifting and rectifying

The lifting jack is installed in the lifting groove during the lifting and rectification process. A steel plate, a tetrafluoroethylene plate (serving as a sliding layer), the lifting jack, and another steel plate are placed in the lifting groove from top to bottom. Once the jack is fully positioned, the lateral constraints of the track are released. All jacks are then lifted synchronously by 10 mm to 15 mm to separate the track structure from the graded gravel beneath the supporting layer. Displacement sensors are installed next to each jack to monitor the lifting amount in real time. A horizontal correction jack (300 kN) and a dial gauge (with 3 m spacing) are placed between each lifting groove to monitor the correction amount in real time. Horizontal jacking is primarily controlled by displacement, with jacking force control as a secondary measure. Pushing at each point stops when the displacement reaches the target value. A total station is used to recheck the horizontal displacement of monitoring points, which are spaced 3 meters apart, once the displacement of all jacking points has reached the target value. The track structure will rebound

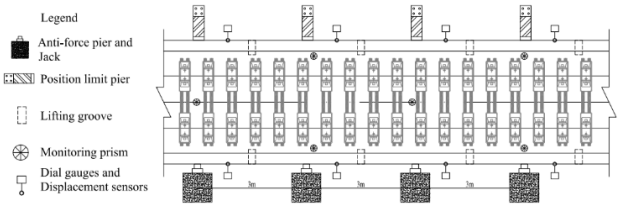

Fig. 12 Layout of the lifting and rectifying system

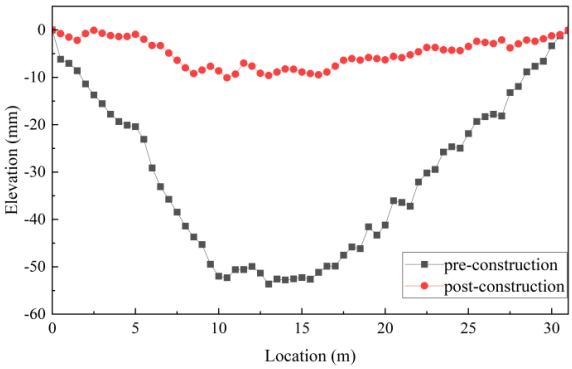

Fig. 13 Comparison of elevation curves before and after construction

during the rectification process. During construction, slight over-correction of 3 mm to 5 mm is required until the alignment meets the design specifications. The layout of the lifting and rectification system is illustrated in Fig. 12.

4.2.5 Position locking of track structure& grouting filling

After the lifting and rectification stage is completed, the slab should be temporarily restrained. Polymer material is then used for grouting to temporarily fill the rectification area, ensuring that the interface voids are densely filled. To prepare for chemical grouting uplift, a tetrafluoroethylene plate is installed between the position limit pier and the side of the supporting layer.

4.2.6 Chemical grouting uplift

The chemical grouting uplift technique for ballastless track involves injecting high polymer material into the graded gravel layer on the subgrade surface via drilled holes. The grouting pressure and expansion force of the high polymer material are used to lift the ballastless track structure, thereby restoring the line regularity. Grouting lifting holes are arranged along the centerline of the slab and supporting layers on both sides, with a spacing of 1.2 m. The drilling depth extends through the subgrade surface layer. The working unit is divided based on the length of the affected area and the available maintenance window. The single lifting amount does not exceed 10 mm, with an electronic level and total station used to monitor both elevation and midline levels. The spacing between elevation monitoring points is 1.2 m, and the prism spacing for midline level monitoring points is 3 m. After lifting is completed, areas with a lifting amount of less than 10 mm are filled with chemical grouting material that has good fluidity and permeability to seal the gaps under the track

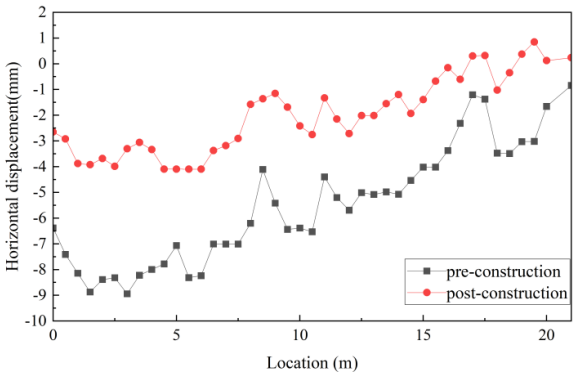

Fig. 14 Comparison of linear horizontal curve before and after construction

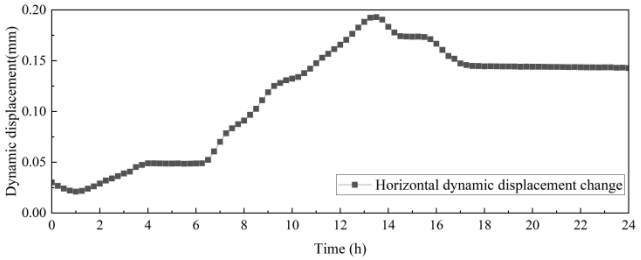

(a) horizontal waveform

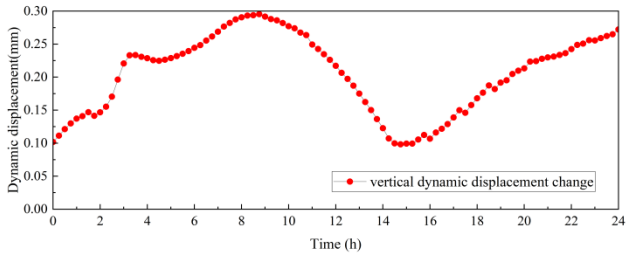

(b) vertical waveform

Fig. 15 Track dynamic displacement waveform

structure. Areas where the lifting amount exceeds 10 mm are filled with polymer mortar.

5. Implementation evaluation

5.1 Track alignment

After the disease area has been lifted and rectified, the alignment of the ballastless track is presented in Figs. 13 and 14. The maximum lifting amount is 39.5 mm, and the maximum deviation correction is 4 mm. Track smoothness has been significantly improved, and the objective of removing non-standard gaskets has been largely achieved. The static geometric dimensions of the track meet the required specifications. However, due to the short length of the rectification area and the rigidity of the concrete, horizontal offsets remain in some sections.

5.2 Track inspection data

According to data from the dynamic inspection vehicle shown in Fig. 16, the peak-to-valley value, horizontal

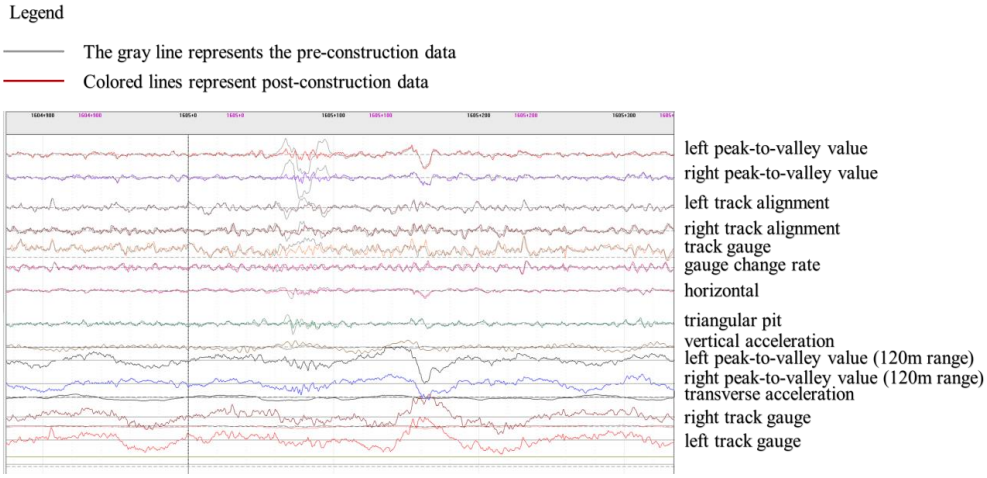

Fig. 16 Measurement results of dynamic inspection vehicle before and after construction

displacement, triangular pit, and vertical acceleration decreased by more than 60% after the lifting and rectification of the disease area. This indicates that the overall rectification scheme effectively addresses the subgrade settlement and track deviation issues.

5.3 Dynamic response

Wireless Linear Variable Displacement Transducer (LVDT) technology is used to monitor the real-time displacement of the track structure. The monitoring results in Fig. 16 show that, when the train passes, the lateral displacement of the track remains below 0.2 mm, and the vertical displacement stays below 0.3 mm. This demonstrates that the track structure remains stable and meets the safety requirements for train operation.

6. Conclusions

The purpose of this study is to develop and validate an innovative approach for addressing subgrade settlement and track deviation issues in high-speed railway double-block ballastless tracks. This approach integrates finite element modeling, mechanical lifting, horizontal correction, and chemical grouting technology to optimize construction parameters and restore track alignment, all while minimizing structural impact.

1. Optimization of Construction Parameters

The dissociation length of the sealing layer between the lines and jack spacing significantly impacts the safety, quality, and efficiency of the overall construction. Simulation results determined that a jack spacing of 3 m and a dissociation length of 31 m effectively reduced jacking force while maintaining track integrity. Increasing the jack spacing beyond 3 m resulted in a 20%–32% increase in jacking force, whereas extending the dissociation length reduced the force per point by approximately 20%.

2. Effectiveness of the Comprehensive Construction Method

Numerical analysis confirmed that multi-point horizontal thrust correction efficiently restored track alignment with minimal rebound effects. The correction process did not induce structural cracking or excessive stress concentrations, ensuring the long-term stability of the track. The engineering case demonstrates that the lifting and rectifying technology for double-block ballastless track structures can resolve subgrade settlement and line deviation issues within the skylight maintenance window.

3. Structural Stability and Long-Term Performance

Post-construction assessments demonstrated a maximum lift of 39.5 mm and a maximum deviation correction of 4 mm, leading to substantial improvements in track smoothness. Dynamic inspection data indicated a >60% reduction in peak-to-valley values, horizontal displacement, and vertical acceleration, confirming compliance with operational safety standards. Wireless Linear Variable Displacement Transducer (LVDT) monitoring verified that lateral and vertical displacements remained below 0.2 mm and 0.3 mm, respectively, under train loading, indicating high structural stability. These results confirm that the applied rectification method effectively maintains track performance over time.

This method provides a reliable solution for railway maintenance, enhancing track durability while the minimizing operational disruptions. The research offers valuable insights for future applications in high-speed railway infrastructure maintenance and repair.

References

Amornfa, K., Quang, H.T. and Tuan, T.V. (2023), "Effect of groundwater level change on piled raft foundation in Ho Chi Minh City, Viet Nam using 3D-FEM", *Geomech. Eng.*, **32**(4), 387-396. https://doi.org/10.12989/gae.2023.32.4.387.

Bian, X., Duan, X., Li, W. and Jiang, J. (2021), "Track settlement restoration of ballastless high-speed railway using polyurethane grouting: Full-scale model testing", *Transport. Geotech.*, **26**, 100381. https://doi.org/10.1016/j.trgeo.2020.100381.

Charoenwong, C., Connolly, D.P., Woodward, P.K., Galvín, P. and Costa, P.A. (2022), "Analytical forecasting of long-term railway track settlement", *Comput. Geotech.*, **143**, 104601.

https://doi.org/10.1016/j.compgeo.2021.104601.
Chen, J., Huang, R., Luo, X., Liao, X. andTang, Q. (2024), "Disintegration process and micro mechanism of mudstone under dry-wet cycles", *Geomech. Eng.*, **36**(1), 9-18. https://doi.org/10.12989/gae.2024.36.1.009.
Cui, X., Zhou, R., Guo, G., Du, B. and Liu, H. (2021), "Effects of differential subgrade settlement on slab track deformation based on a DEM-FDM coupled approach", *Appl. Sci.*, **11**(4), 1384. https://doi.org/10.3390/app11041384.
Dong, W., Wang, X., He, Q. and Ren, J. (2022), "A survey of Ballastless track defects in China's high-speed railway after ten years of service", *Intell. Transport. Infrastruct.*, **1**, 1-16. https://doi.org/10.1093/iti/liac023.
Ghofrani, F., He, Q., Goverde, R.M. and Liu, X. (2018), "Recent applications of big data analytics in railway transportation systems: A survey", *Transport. Res. Part C: Emerging Technol.*, **90**, 226-246. https://doi.org/10.1016/j.trc.2018.03.010.
Giunta, M. and Praticò, F.G. (2017), "Design and maintenance of high-speed rail tracks: A comparison between ballasted and ballast-less solutions based on life cycle cost analysis", *Transport Infrastructure and Systems*, CRC Press, 87-94. https://doi.org/10.1201/9781315281896-14.
Hadi, M.A., Alzabeebee, S. and Keawsawasvong, S. (2023), "Three-dimensional finite element analysis of the interference of adjacent moving trains resting on a ballasted railway track system", *Geomech. Eng.*, **32**(5), 483-494. https://doi.org/10.12989/gae.2023.32.5.483.
Hu, G., Xia, Y., Zhong, L., Ruan, X. and Li, H. (2023), "Study on collapse mechanism and treatment measures of portal slope of a high-speed railway tunnel", *Geomech. Eng.*, **32**(1), 111-123. https://doi.org/10.12989/gae.2023.32.1.111.
Lawrence, M., Bullock, R. and Liu, Z. (2019), *China's High-Speed Rail Development*. World Bank Publications.
Liu, H., Liu, J., Jiang, Z., Wang, H., Zhang, Y., Song, S. and Li, Y. (2021), "Research on the deformation behaviour of the track interlayer structure during the deviation correction of the offset ballastless Track", *IOP Conference Series: Earth and Environmental Science* **719**(3), 032083. https://doi.org/10.1088/1755-1315/719/3/032083.
Ngamkhanong, C., Feng, B., Tutumluer, E., Hashash, Y.M. and Kaewunruen, S. (2021) , "Evaluation of lateral stability of railway tracks due to ballast degradation", *Constr. Build. Mater.*, **278**, 122342. https://doi.org/10.1016/j.conbuildmat.2021.122342.
Nguyen, A.D., Nguyen, V.T. and Kim, Y.S. (2023), "Finite element analysis on dynamic behavior of sheet pile quay wall dredged and improved seaside subsoil using cement deep mixing", *Int. J. Geo-Eng.*, **14**(1), 9. https://doi.org/10.1186/s40703-023-00186-x.
Nobakht, S., Zakeri, J.A. and Safizadeh, A. (2022), "Investigation on longitudinal resistance of the ballasted railway track under vertical load", *Constr. Build. Mater.*, **317**, 126074. https://doi.org/10.1016/j.conbuildmat.2021.126074.
Paixão, A., Fortunato, E. and Calçada, R. (2015), "The effect of differential settlements on the dynamic response of the train–track system: A numerical study", *Eng. Struct.*, **88**, 216-224. https://doi.org/10.1016/j.engstruct.2015.01.044.
Ren, J., Deng, S., Zhang, K., Du, W. and Wu, Q. (2021), "Design theories and maintenance technologies of slab tracks for high-speed railways in China: a review", *Transport. Saf. Environ*., (4), tdab024. https://doi.org/10.1093/tse/tdab024.
Scheweiger, H.F., Kummerer, C., Otterbein, R. and Falk, E. (2004), "Numerical modeling of settlement compensation by means of fracture grouting", *Soils Found.*, **44**(1), 71-86. https://doi.org/10.3208/sandf.44.71.
Song, B., Liu, J. Y., Liu, Y. and Hu, P. (2024), "Generalization and implementation of hardening soil constitutive model in ABAQUS code", *Geomech. Eng.*, **36**(4), 355-366. https://doi.org/10.12989/gae.2024.36.4.355.
Zamani, S., Lajevardi, S.H., Yarivand, A. and Zeighami, E. (2023), "Experimental study of the behavior of square footing on reinforced sand with treated geotextile", *Int. J. Geo-Eng.*, **14**(1), 19. https://doi.org/10.1186/s40703-023-00195-w.
Zeng, Z., Xiao, Y., Wang, W., Huang, Z., Wei, W. and Houdou, S. B. (2022) , "Research on dynamic performance of CRTSIII type slab ballastless track under long-term service", *Materials*, **15**(6), 2033. https://doi.org/10.3390/ma15062033.
Zeng, Z., Ye, M., Wang, W., Liu, J., Shen, S. and Qahtan, A.A.S. (2022), "Analysis on mechanical characteristics of CRTSII slab ballastless track structures in rectification considering material brittleness", *Constr. Build. Mater.*, **319**, 126058. https://doi.org/10.1016/j.conbuildmat.2021.126058.
Zuo, S., Li, T., Li, J., Liu, P. and Cui, X. (2022), "Research on dynamic response and construction safety countermeasures of an adjacent existing line foundation under the influence of a new railway line", *Coatings*, **12**, 641. https://doi.org/10.3390/coatings12050641.